Am J Cancer Res 2011;1(2):144-154
www.ajcr.us /ISSN:2156-6976/ajcr0000016

Original Article

Direct evidence for lineage-dependent effects of bone marrow stromal cells on tumor progression

Michelle R. Dawson[1], Sung-Suk Chae, Rakesh K. Jain, Dan G. Duda

Steele Laboratory for Tumor Biology, Massachusetts General Hospital, Harvard Medical School, Boston, MA, USA. [1]Current address: Department of Chemical and Biomolecular Engineering, Georgia Institute of Technology, Atlanta, GA, USA.

Received December 3, 2010; accepted December 6, 2010; Epub: December 6, 2010; Published January 1, 2011

Abstract: We sought to characterize the function of bone marrow stromal cell (BMSC) populations in tumor progression. Because this function may depend on the cell-lineage and mouse strain heterogeneity, we first characterized *ex vivo* the BMSCs harvested from C57BL/6 versus FVB mice and established their *in vivo* function in tumor growth and metastasis experiments. All plastic-adherent BMSCs expressed platelet-derived growth factor receptor beta (PDGFRβ) and stem cell antigen 1 (Sca1), consistent with a mesenchymal precursor phenotype, as well as CD80. Moreover, these BMSCs were capable of differentiation along mesenchymal lineage into adipocytes, osteoblasts, chondrocytes or myofibroblasts. However, further phenotypic analysis detected a distinct populations of myeloid ($CD11b^+$) precursor cells amongst the *ex vivo* expanded BMSCs –with specific surface marker phenotypes and gene expression pattern. When co-implanted with metastatic cancer cells, all the BMSCs persisted and integrated into tumor stroma, but only myeloid BMSCs significantly promoted tumor growth and metastasis. These data demonstrate the differential effect of BMSCs sub-populations on tumor progression. These results may have important implications for anti-tumor therapy and for the use of mesenchymal BMSCs as cell-based therapies.

Keywords: Myeloid, mesenchymal, bone marrow-derived cells, tumor, metastasis

Introduction

Bone marrow stromal cells (BMSCs) are multipotent progenitors that can self-renew and differentiate into multiple cell types, including adipocytes, osteoblasts, and chondrocytes. Recent studies have shown that BMSCs harvested from humans or mice can be expanded and genetically engineered while preserving cell multipotency without malignant transformation [1-4]. These properties make BMSCs extremely attractive for cell-based therapies. However, at least three important caveats remain, (i) the inter-strain heterogeneity in the yield of BMSCs; and (ii) the contamination with cells of non-mesenchymal lineage, e.g., myeloid ($CD11b^+$) cells; and (iii) the potential immunosuppressive effects of mesenchymal BMSCs [3, 5].

In addition, BMSCs can spontaneously infiltrate endocrine pancreatic tumors and differentiate to myofibroblasts [6]. *Ex vivo* expanded mesenchymal BMSCs can also engraft into tumors. For example, human BMSCs have been shown to promote metastasis in a xenograft model of human breast cancer in immunodeficient mice [7]. However, certain myeloid ($CD11b^+$) BMSCs–that express mesenchymal markers such as PDGFRβ or NG2–also infiltrate tumors or injured tissues [8-11]. Therefore, establishing the specific roles of mesenchymal versus myelomonocytic BMSCs requires unambiguous identification of each BMSC population. Here, we dissected the phenotype of BMSCs and the role of distinct BMSC sub-populations on tumor progression in immunocompetent mice of different strain background.

Materials and methods

BMSC harvest and culture methods

BMSCs were obtained from femurs and tibias of mice using an established protocol [12]. Briefly,

primary bone marrow cells were cultured in Mesencult or Iscove's Modified Dulbecco's (IMDM) medium (Stem Cell Technologies, Canada) in plastic dishes to confluence. We used an established colony-forming unit fibroblast assay to characterize the surface phenotype and the differentiation of BMSCs [3]. BMSCs seeded at 25-5000 cells per well in 24-well plates were cultured in Mesencult medium for 14 days, fixed in methanol, and stained with crystal violet. For differentiation assays, BMSCs expanded *ex vivo* for 3-8 passages were cultured in differentiation media for 2-4 weeks and stained with Alizarin red (for osteoblasts), Oil Red-O (for adipocytes), Alcian blue (for chondrocytes) or anti-αSMA and NG2 (for fibroblasts), as previously described [3, 13, 14]. For *in vivo* experiments, we isolated and expanded GFP$^+$ BMSCs from transgenic mice (n=10 per group) expressing GFP constitutively (*EF1α-GFP*/FVB mice and *Actb-GFP*/C57BL/6 mice)[12, 15, 16]. LA-P2097 mouse lung carcinoma cells (syngeneic to FVB mice, established in the Steele Laboratory [16]) and Lewis lung carcinoma cells (LLC1), purchased from ATCC (Manassas, VA) were cultured in DMEM supplemented with 10% FCS.

Phenotypic analysis using flow cytometry

The surface phenotype of plastic-adherent BMSCs isolated from the bone marrow of C57BL/6, *Actb-GFP*/C57BL/6, FVB and *EF1α-GFP*/FVB mice was investigated by immunostaining and cytometric analyses using a LSR-II flow cytometer. Briefly, cultured BMSCs (passage 1, 3 or 20) were separated into 100μl aliquots and labeled with 2% PerCP-CD45, PE-Sca1, APC-CD11b, APC-Cy7(AF750)-CD80, PE-F4/80, APC-Cy7(AF750)-PDGFRb, APC-CD31 and APC-Cy7(AF750) Gr-1 antibodies. There were no differences between the phenotypes of BMSCs from C57BL/6 and *Actb-GFP*/C57BL/6 or between the BMSCs from FVB and *EF1α-GFP*/FVB mice, respectively. Thus, BMSCs constitutively expressing GFP (from *EF1α-GFP*/FVB and *Actb-GFP*/C57BL/6 mice) were used for *in vivo* studies.

Evaluation of the role of BMSCs in tumors in vivo

We co-implanted BMSCs (passage 3) at a 1:1 ratio with metastatic lung carcinoma cells either subcutaneously (s.c., 3 x 10^5 cells of each type) or in dorsal skinfold chambers (DSC, 2 x 10^5 cells of each type), as previously described [12, 15-17]. FVB mouse-derived BMSCs were co-implanted with LA-P2097 and C57BL/6 mouse-derived BMSCs were co-implanted with LA-P2097 (n=6 in DSC and n=10 s.c.). Intravital multiphoton laser-scanning microscopy was used to study and quantify the engraftment of the GFP$^+$ BMSCs in tumors, as previously described [18]. S.c. tumors were measured twice weekly using a caliper, and were resected when they reached a diameter of 10mm to induce formation of metastases in the lungs [12, 17, 19]. All tumor tissues were collected for analysis by immunohistochemistry at the end of the experiments.

RNA extraction and cDNA synthesis, oligonucleotide array, and qRT-PCR

RNA was isolated from adherent *EF1α-GFP*/FVB (passage 3), *Actb-GFP*/C57BL/6 (passage 3), or C57BL/6 (passage 20) bone marrow derived cells (n=4) using TRIzol reagent (Life Technologies, Inc., Rockville, MD) according to the manufacturer's specifications. Qiagen RNeasy® Mini Kit was used to extract RNA prior to cDNA synthesis. cDNA was prepared for qRT-PCR and oligonucleotide arrays using the Thermoscript RNA PCR kit from Invitrogen. Oligonucleotide arrays were performed on cDNA extracted from cells that were isolated with the bone marrow cells used in our animal studies. This cDNA, along with cDNA extracted from three additional bone marrow collections, was used for qRT-PCR. The expression of angiogenesis genes in BMSCs from *EF1α-GFP*/FVB (passage 3), *Actb-GFP*/C57BL/6 (passage 3), or C57BL/6 (passage 20) was profiled using a mouse angiogenesis PCR oligonucleotide array (SA Biosciences, PAMM-024) according to manufacturer's protocol. For qRT-PCR, SYBR green and LUX primers were designed with Primer Express Software (Applied Biosystems). Primers used in our study included: mGAPDH, mMMP9, mMMP2, mCTGF, mTNFα, mCXCL2, mCXCL1, mCCL2, mTie2, mIL1β, mIL6, mThbs1, mThbs2, and mHIF1α. Samples were run on the Applied Biosystems 7000 Sequence Detection System. Mouse GADPH was used as a qRT-PCR control.

Myeloid cell isolation and co-implantation with tumor cells

CD11b$^+$ cells were isolated from whole bone marrow harvested from *EF1α-GFP*/FVB mice or *Actb-GFP*/C57BL/6 mice (n=8) by negative se-

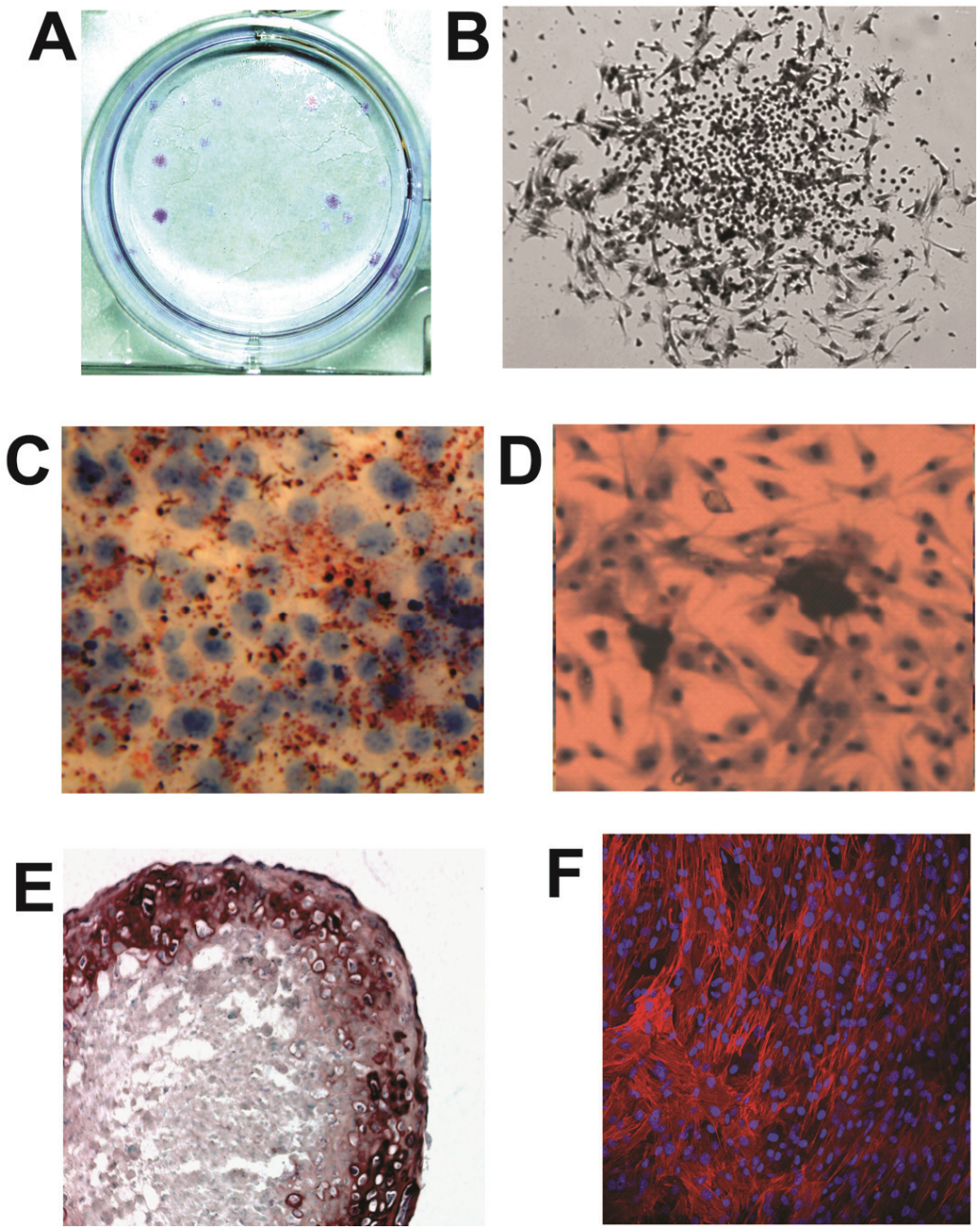

Figure 1. *Ex vivo* expansion and differentiation of BMSCs. **A,B,** Colony formation assay (crystal violet staining). **C-F**, Differentiation assay for BMSCs into: adipocytes (Oil Red-O staining in **C**), chondrocytes (Alcian blue staining in **D**), osteoblasts (Alizarin red in **E**), and fibroblasts (Cy3-anti-αSMA Ab in **F**).

lection using magnetic bead separation techniques. Mice were sacrificed by cervical dislocation and the tibiae and femurs were removed and flushed with cold PBS containing 5% fetal bovine serum. Bone marrow cells were centrifuged, filtered and re-suspended in 10 ml of sterile PBS. Two hundred microliters of biotinylated mouse lineage cocktail, containing equal volumes of TER-119 (Ly-76), Gr-1 (Ly-6G/C), CD45R (B220), and CD3e, were added (BD Pharmingen, San Jose, CA, Product number 559971). The cells were incubated on ice for 30 minutes and 400 μl of Biotin-Binding Dynabeads (Invitrogen, Carlsbad, CA, Product

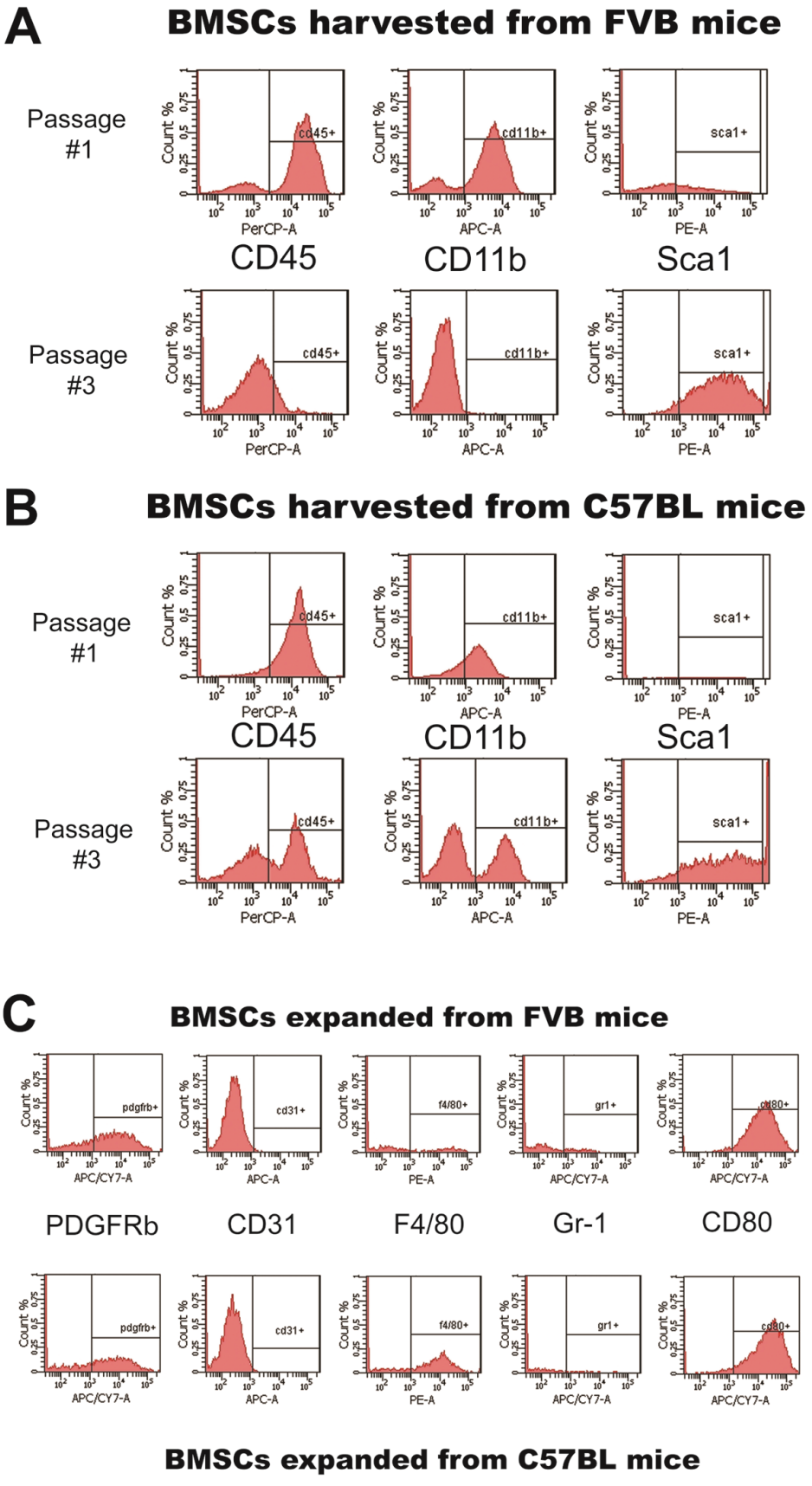

Figure 2. Differential phenotype of plastic-adherent BMSCs from FVB and C57BL/6 mice. **A-C**, Flow cytometric analyses performed after first and third passage of BMSCs from FVB mice (**B**) or C57BL/6 mice (**B**) immunostained with PerCP-CD45, PE-Sca1, APC-CD11b, APC-Cy7-CD80, PE-F4/80, APC-Cy7-PDGFRb, APC-CD31 and APC-Gr-1 antibodies. The BMSCs expanded from C57BL/6 mice contain myeloid cells that are PDGFRβ+CD31−F4/80+Gr-1−CD80+ (**C**).

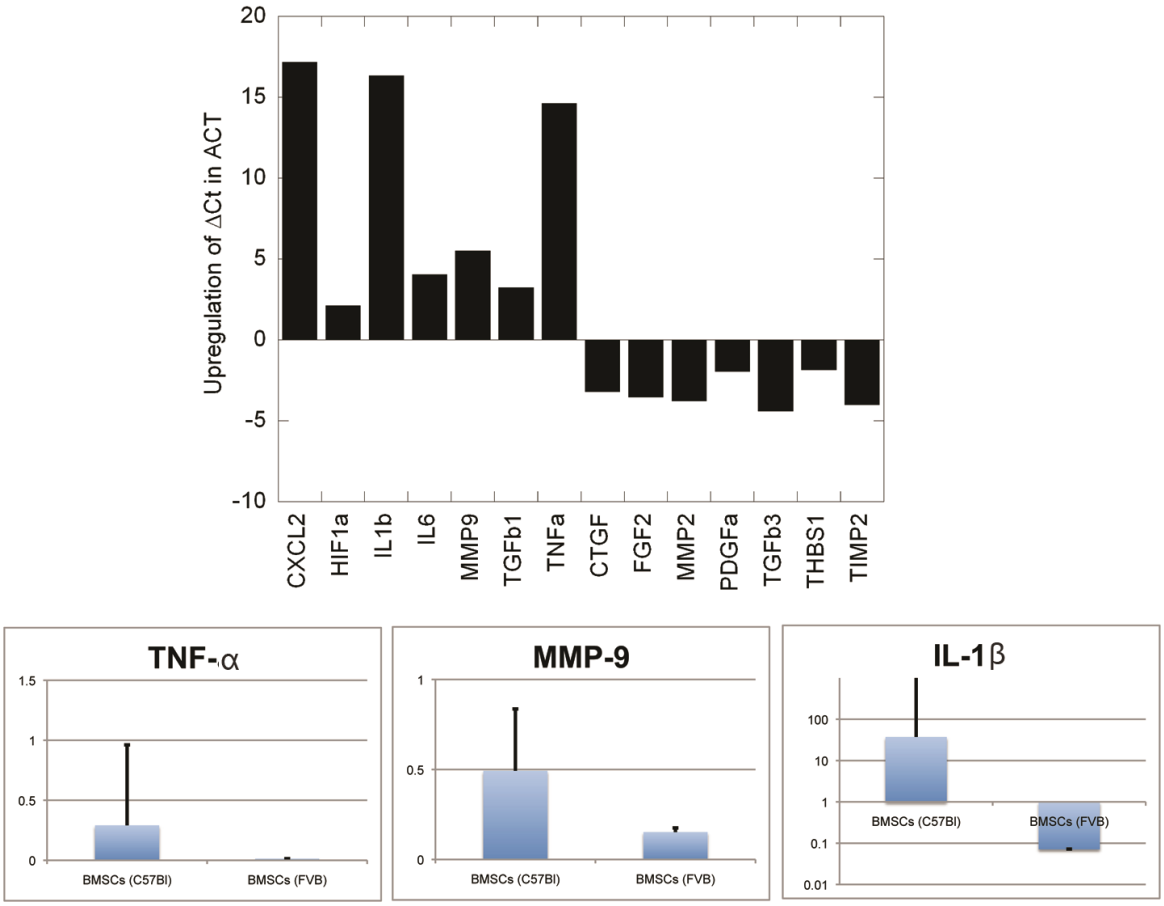

Figure 3. Differential gene expression between mesenchymal and myeloid BMSCs. Data are shown as fold difference in gene expression, normalized by beta-actin (for PCR array) and GAPDH (for qPCR evaluation of TNF-α, MMP-9 and IL -1β).

number 110-47) were added. The cells were placed on a rocker and incubated for an additional 45 minutes on a shaker plate at 4°C. Cells were separated into 5 ml aliquots and the MCP-1 magnet was used for magnetic bead depletion (depletion step was repeated 4 times). Cells were centrifuged and resuspended in 2 ml PBS. Red blood cells were lysed using 5 ml ACK buffer. Cells were centrifuged and resuspended in a small volume of PBS. This procedure yielded approximately 2 million cells. Flow cytometry was used to confirm that more than 98% of the cells were positive for CD11b and negative for TER-119, Gr-1, CD45R, and CD3e. $CD11b^+$ (myeloid) cells from FVB or C57BL/6 mice were co-implanted with syngeneic LA-P0297 or LLC1 tumor cells in immunocompetent mice or with LLC1 cells in SCID mice at a 1:1 ratio (n=8 mice per group, 250,000 tumor cells per mouse). Tumor growth was monitored as described above.

Statistical analysis

Subcutaneous and dorsal skinfold tumor studies were performed with 6-8 mice per group. Pooled bone marrow from 8-10 mice per group was used for flow cytometry and oligonucleotide analysis. For qRT-PCR analysis, RNA was isolated from pooled or single-animal collections of bone marrow. Data reported is from single animal bone marrow collections (n=3); however, there were no statistical differences between qRT-PCR analysis for pooled bone marrow versus single animal isolated bone marrow. Flow cytometry experiments were repeated at least 3 times. Student's t-test was used to compare experimental groups and a $p < 0.05$ designated

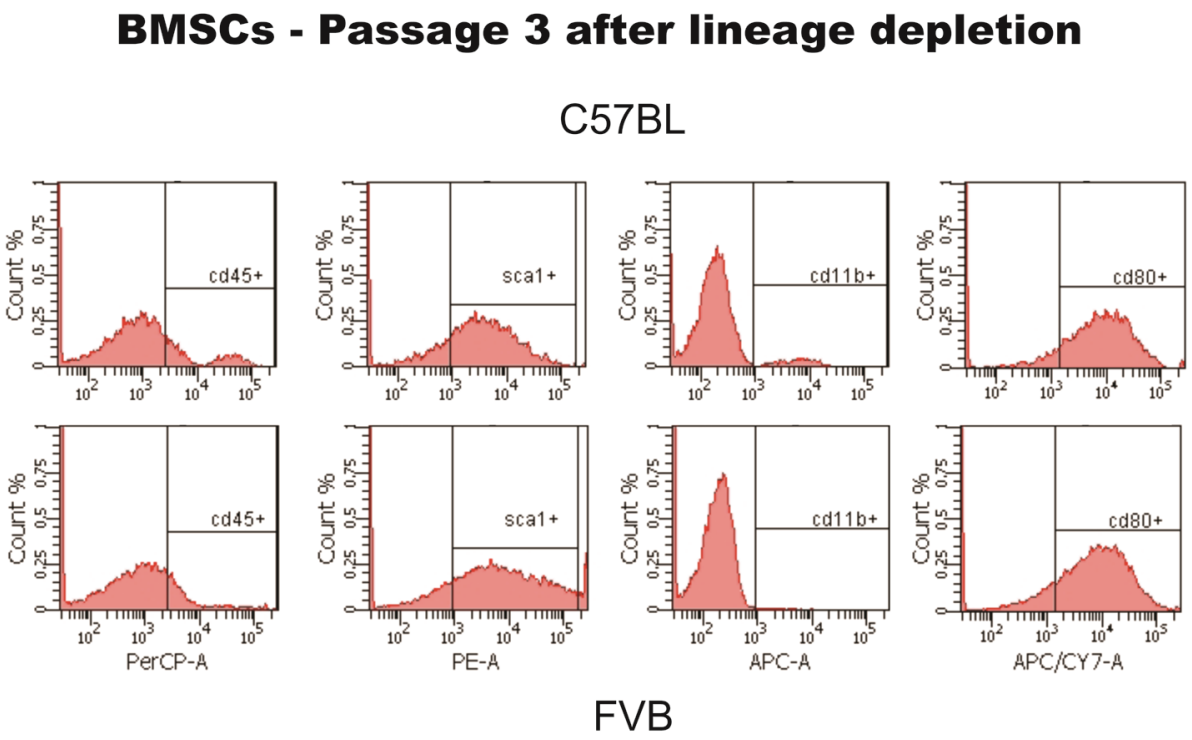

Figure 4. Phenotype of purified mesenchymal BMSCs from C57BL/6 mice. Flow cytometric analyses performed after third passage of BMSCs immunostained with PerCP-CD45, PE-Sca1, APC-CD11b and APC-Cy7-CD80 antibodies confirmed that all the expanded BMSCs are of mesenchymal lineage.

a statistically significant difference. The rates of spontaneous metastasis formation were compared using the Mann-Whitney U test (Wilcoxon rank-sum test).

Results and discussion

Plastic-adherent BMSCs are a heterogenous population of mesenchymal and myeloid cells

BMSCs expanded *in vitro* as adherent cell colonies measuring 1-2 mm in diameter and displayed heterogeneous morphology (**Figure 1A,B**). The optimal density for BMSC expansion was 125 cells/well, and resulted in the formation of single colonies. As expected, cells among the expanded BMSCs differentiated into osteoblasts, adipocytes, chondrocytes and fibroblasts (**Figure 1C-F**).

However, given the heterogeneous morphology of BMSCs, we characterized their surface phenotype at first *in vitro* passage and after 3 passages. At first passage, the majority of the adherent BMSCs displayed a myelomonocytic phenotype ($CD45^+CD11b^+Sca1^-$) in both FVB and C57BL/6 mice (**Figure 2A,B**). After three passages, the cultured cells were substantially enriched in $Sca1^+$ progenitor BMSCs, as determined by both flow cytometry and immunocytochemistry (**Figure 2A,B** and not shown). However, whereas BMSCs from FVB mice displayed a characteristic mesenchymal BMSC phenotype ($Sca1^+Gr\text{-}1^-F4/80^-CD11b^-CD31^-CD45^-$), the BMSCs from C57BL/6 mice contained a mixture of adherent mesenchymal and myelomonocytic cells ($Sca1^+CD11b^+F4/80^+CD45^+CD31^-Gr\text{-}1^-$, **Figure 2C**). Surprisingly, all the BMSCs expressed the co-stimulatory molecule CD80 and the mesenchymal-selective marker $PDGFR\beta^+$ (**Figure 2D**). In addition, PCR array and qPCR confirmed the increased expression of several genes–typically expressed by myeloid cells–in the C57BL/6 mouse-derived BMSCs, including CXCL2/macrophage inflammatory protein 2-alpha (MIP2-α), Interleukin (IL)-1β, IL-6, tumor necrosis factor alpha (TNF-α) and matrix-metalloproteinase 9 (MMP9) (**Figure 3**). Of note, myeloid cell-derived IL-1β and MMP-9 have been previously shown to mediate carcinogene-

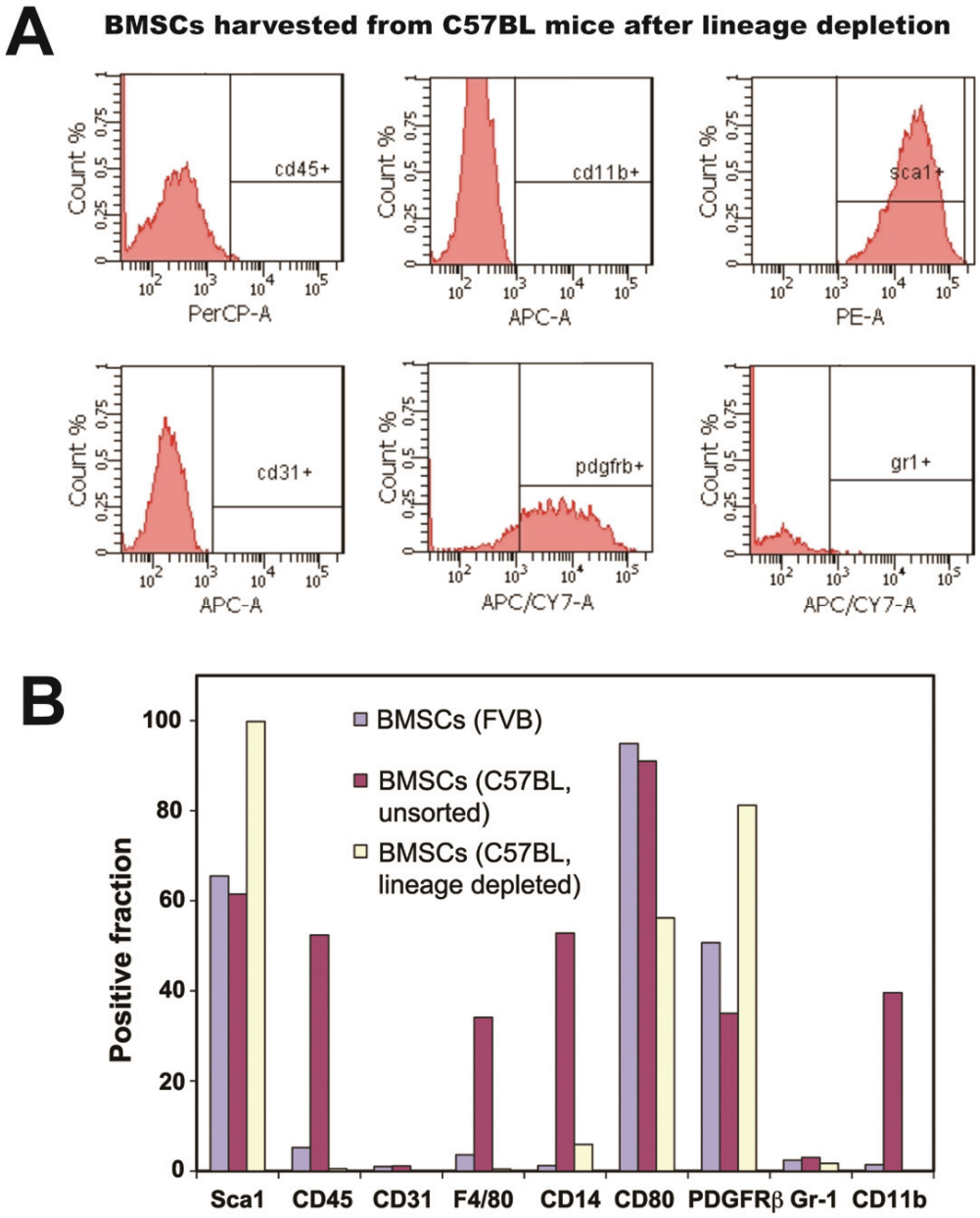

Figure 5. Phenotype of late passage BMSCs from C57BL/6 and FVB mice. **A**, Flow cytometric analyses performed after twenty passages of BMSCs immunostained with PerCP-CD45, PE-Sca1, APC-CD11b, APC-Cy7-CD80, APC-CD31 and APC-Gr-1 antibodies confirmed that the C57BL/6-derived BMSCs are mesenchymal precursors. **B**, Phenotype of late passage BMSCs from FVB mice (unsorted) and from C57BL/6 with or without prior purification for mesenchymal BMSC expansion.

sis and tumor growth [20, 21]. Collectively, these data demonstrate myeloid progenitor cell contamination amongst adherent BMSCs and an inter-strain heterogeneity in phenotype. We next evaluated the functional significance of this heterogeneity.

Myeloid BMSCs promote the differentiation of mesenchymal BMSCs

To this end, we first evaluated whether the contaminating myelomonocytic BMSCs influence mesenchymal BMSC renewal and differentia-

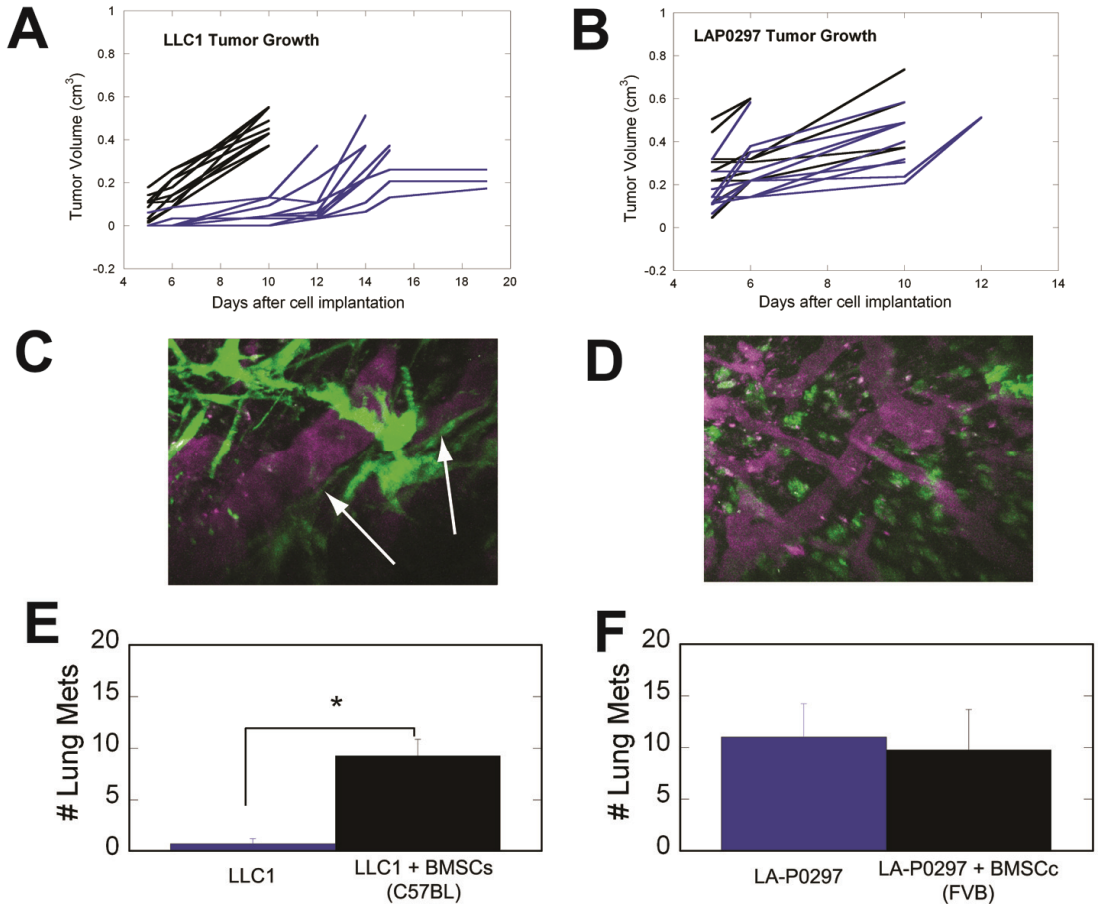

Figure 6. Differential *in vivo* phenotype and tumor-promoting effects of BMSCs from FVB and C57BL/6 mice. **A,B,** Effect of BMSCs on primary tumor growth: C57BL/6-mouse-derived BMSCs (largely myelomonocytic) significantly accelerate the early growth of LLC1 tumors (**A**), whereas FVB mouse-derived BMSCs do not significantly affect LA-P0297 growth in syngeneic mice (**B**). **C,D,** Effect of BMSCs on lung metastasis after primary tumor resection: The number of metastases is significantly higher in mice co-implanted with C57BL/6-mouse-derived BMSCs and LLC1 cells versus LLC1 alone (**C**), but not in mice co-implanted with the FVB mouse-derived BMSCs and LA-P0297 versus LA-P0297 alone (**D**). **E,F,** Representative *in vivo* microscopy images of BMSCs engrafted in tumors: C57BL/6-mouse-derived BMSCs show a round-shape characteristic for myeloid cells (**E**), whereas FVB mouse-derived BMSCs have a mesenchymal appearance (**F**).

tion. C57BL/6 mouse-derived BMSC culture led to rapid terminal differentiation of the mesenchymal BMSCs into αSMA$^+$ fibroblasts. In contrast, depletion of hematopoietic BMSCs (using a lineage marker antibody cocktail) allowed expansion of purified Sca-1$^+$CD45$^-$ mesenchymal BMSCs from C57BL/6 mice similar to FVB mice (**Figure 4**). These BMSCs showed no elevation in myeloid cell-specific surface markers or genes (**Figure 5A** and not shown). Endothelial cells were also detectable by flow cytometry in fresh bone marrow samples, and had a similar Sca-1$^+$CD45$^-$ phenotype, but were also CD31^{bright} (not shown) and did not expand in the Mesencult media (**Figure 5**).

Myeloid BMSCs promote tumor growth and progression to metastasis

In addition, taking advantage of this inter-strain heterogeneity in BMSC phenotypes, we characterized the specific roles of the mesenchymal and myelomonocytic BMSC subpopulations in tumor progression using established models in immunocompetent mice. GFP-labeled BMSCs isolated from FVB or C57BL/6 mice and ex-

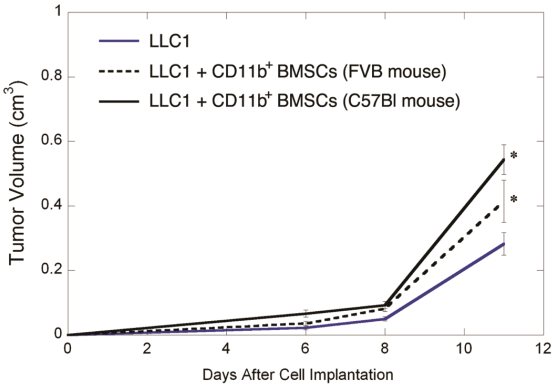

Figure 7. Tumor-promoting effects of myeloid BMSCs from mice of different strains. Co-implantation of myeloid ($CD11b^+$) BMSCs from both C57BL/6 and FVB mice accelerated LLC1 growth in SCID mice.

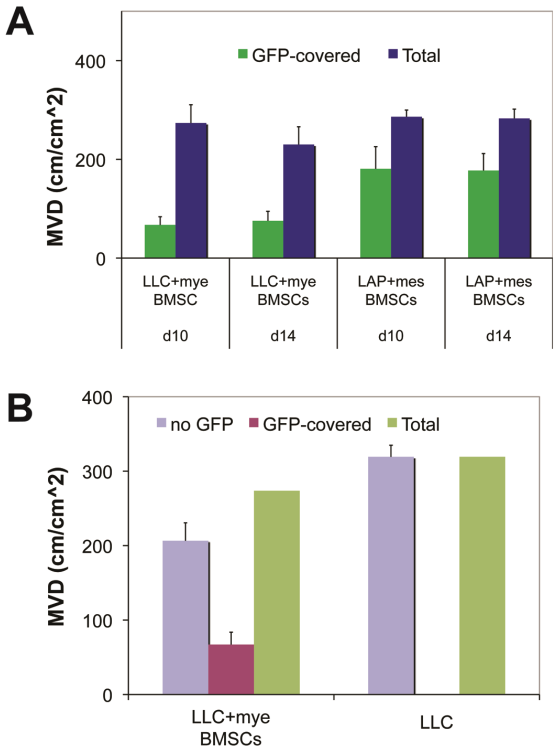

Figure 8. Interaction between BMSCs from FVB and C57BL/6 mice with tumor vasculature at days 10 and 14 after co-implantation with LA-P0297 (LAP) or LLC cells, respectively. **A.** Association between BMSCs from C57BL/6 mice (primarily of myeloid lineage– mye BMSCs) and from FVB mice (largely mesenchymal– mes BMSCs): The vessel coverage by GFP^+ BMSCs is significantly increased for mesenchymal BMSCs from FVB mice. **B.** Co-implantation of myeloid BMSCs does not significantly change tumor microvascular density (MVD).

panded for three passages were co-implanted with lung carcinoma cells LA-P0297 (in FVB mice) and LLC1 (in C57BL/6 mice). Subcutaneous tumor growth was compared to cancer cell implantation alone (n=10). Co-implantation of BMSCs from C57BL/6 mice (rich in myelomonocytic BMSCs) significantly increased LLC1 tumor growth compared to implantation of LLC1 alone ($p<0.05$, **Figure 6A**). In contrast, co-implantation of BMSCs from FVB mice did not significantly change the growth kinetics of LA-P0297 (**Figure 6B**). Moreover, the number of lung metastases– spontaneously formed two weeks after resection of the tumors when they reached a diameter of 1cm–was significantly higher in mice co-implanted with C57BL/6 mouse-derived BMSCs and LLC1 compared to those implanted with LLC1 alone ($p<0.05$, **Figure 6C**). In contrast, co-implantation of FVB mouse-derived BMSCs with LA-P0297 had no impact on the number of metastases (**Figure 6D**).

To confirm the role of myelomonocytic BMSCs in tumor growth enhancement, we sorted $CD11b^+$ BMSCs from FVB mice and co-implanted them with LLC1 cells in immunodeficient (SCID) mice (n=8). The myelomononocytic BMSCs from FVB mice significantly enhanced LLC1 and LA-P0297 tumor growth, similar to C57BL/6 mouse-derived BMSCs (**Figure 7** and not shown, $p<0.05$). Collectively, these data are consistent with a tumor-promoting effect of the myeloid BMSCs, i.e., generation of progeny with M2-type activation [22]. This provides a useful model for the study of bone marrow-derived cells in the early phases of tumor growth and metastasis, which has been unambiguously shown in models of genetic deficiency in MMP-9 and TNF-α/TLR2 [20, 23].

To dissect the differential role of mesenchymal versus myelomonocytic BMSCs in tumor angiogenesis, we co-implanted C57BL/6 mouse-derived BMSCs with LLC1 cells and FVB mouse-derived BMSCs with LA-P0297 cells in dorsal skin-fold chamber windows (n=6). Using intravital MPLSM, we found that BMSCs incorporated into the growing tumor and persisted for the two weeks of observation. Of the detectable FVB mouse-derived BMSCs, the majority (62% ± 9%) wrapped around functional vessels as perivas-

cular cells and the rest closely interacted with collagen fibers at the periphery of LA-P0297 tumors– all with typical mesenchymal morphology (**Figure 6E** and **Figure 8A**). In contrast, a significantly smaller fraction of the C57BL/6 mouse-derived BMSCs covered the LLC1 tumor vessels as perivascular cells (32% ± 4%, $p<0.05$), whereas the majority was represented small, round-shaped myeloid cells localized in the tumor stroma (**Figure 6F** and **Figure 8A**). Moreover, the co-implantation of myeloid BMSCs did not change the tumor microvascular density (**Figure 8A**). Collectively, these data indicate that myeloid BMSCs promote primary tumor growth and metastasis likely via paracrine interactions with the cancer cells and the vasculature, without changing the microvascular density.

Conclusions and implications

In summary, we employed methods that allow harvesting and expansion of BMSCs to characterize their phenotype and gene expression *ex vivo* and their effect on tumor growth and metastasis *in vivo*. We found that plastic-adherent myeloid BMSCs share PDGFRβ and CD80 expression with mesenchymal BMSC, but retain myeloid cell characteristics. Moreover, we show that these myelomonocytic BMSCs significantly accelerate tumor growth and metastasis in immunocompetent mice. On the other hand, mesenchymal BMSCs did not accelerate growth. Collectively, these findings offer direct evidence for a differential role of BMSC subsets in tumor progression. In addition, this model will allow further dissection of the role of myeloid BMSCs and their progeny in tumor milieu. These findings may have important implications for the use of these cells as vehicle for therapeutics, or as potential targets for anti-tumor and anti-metastasis therapy.

Acknowledgments

We wish to acknowledge the outstanding technical assistance of J Kahn, S Roberge and P Huang with animal models, and the statistical support from M Ancukiewicz. Grant support: National Cancer Institute grants P01-CA80124, R01-CA115767, R01-CA85140, R01-CA126642 and T32-CA73479 (RKJ), Federal Share Proton Beam Program grants (RKJ and DGD), and R21-CA139168 (DGD), and ACS grant RSG-11-073-01TBG and Spiro Research Awards (DGD).

Please address correspondence to: Dan G. Duda, DMD, PhD, 100 Blossom Street, Cox-734, Steele Laboratory, Massachusetts General Hospital, Boston, MA 02114. Phone 617-726-4648; Fax: 617-726-1962; E-mail: duda@steele.mgh.harvard.edu

References

[1] Oliner J, Min H, Leal J, Yu D, Rao S, You E, Tang X, Kim H, Meyer S, Han SJ, Hawkins N, Rosenfeld R, Davy E, Graham K, Jacobsen F, Stevenson S, Ho J, Chen Q, Hartmann T, Michaels M, Kelley M, Li L, Sitney K, Martin F, Sun JR, Zhang N, Lu J, Estrada J, Kumar R, Coxon A, Kaufman S, Pretorius J, Scully S, Cattley R, Payton M, Coats S, Nguyen L, Desilva B, Ndifor A, Hayward I, Radinsky R, Boone T and Kendall R. Suppression of angiogenesis and tumor growth by selective inhibition of angiopoietin-2. Cancer Cell 2004; 6: 507-516.

[2] Kobune M, Kawano Y, Ito Y, Chiba H, Nakamura K, Tsuda H, Sasaki K, Dehari H, Uchida H, Honmou O, Takahashi S, Bizen A, Takimoto R, Matsunaga T, Kato J, Kato K, Houkin K, Niitsu Y and Hamada H. Telomerized human multipotent mesenchymal cells can differentiate into hematopoietic and cobblestone area-supporting cells. Exp Hematol 2003; 31: 715-722.

[3] Peister A, Mellad JA, Larson BL, Hall BM, Gibson LF and Prockop DJ. Adult stem cells from bone marrow (MSCs) isolated from different strains of inbred mice vary in surface epitopes, rates of proliferation, and differentiation potential. Blood 2004; 103: 1662-1668.

[4] Bernardo ME, Zaffaroni N, Novara F, Cometa AM, Avanzini MA, Moretta A, Montagna D, Maccario R, Villa R, Daidone MG, Zuffardi O and Locatelli F. Human bone marrow derived mesenchymal stem cells do not undergo transformation after long-term in vitro culture and do not exhibit telomere maintenance mechanisms. Cancer Res 2007; 67: 9142-9149.

[5] Phinney DG, Kopen G, Isaacson RL and Prockop DJ. Plastic adherent stromal cells from the bone marrow of commonly used strains of inbred mice: Variations in yield, growth, and differentiation. Journal of Cellular Biochemistry 1999; 72: 570-585.

[6] Direkze NC, Hodivala-Dilke K, Jeffery R, Hunt T, Poulsom R, Oukrif D, Alison MR and Wright NA. Bone marrow contribution to tumor associated myofibroblasts and fibroblasts. Cancer Res 2004; 64: 8485-8794.

[7] Karnoub AE, Dash AB, Vo AP, Sullivan A, Brooks MW, Bell GW, Richardson AL, Polyak K, Tubo R and Weinberg RA. Mesenchymal stem cells within tumour stroma promote breast cancer metastasis. Nature 2007; 449: 557-563.

[8] Rajantie I, Ilmonen M, Alminaite A, Ozerdem U, Alitalo K and Salven P. Adult bone marrow-derived cells recruited during angiogenesis com-

prise precursors for periendothelial vascular mural cells. Blood 2004; 104: 2084-2086.
[9] Song S, Ewald AJ, Stallcup W, Werb Z and Bergers G. PDGFRbeta+ perivascular progenitor cells in tumours regulate pericyte differentiation and vascular survival. Nat Cell Biol 2005; 7: 870-879.
[10] Jones R, Capen DE, Jacobson M, Cohen KS, Scadden DT and Duda DG. VEGFR2PDGFRbeta circulating precursor cells participate in capillary restoration after hyperoxia acute lung injury (HALI). J Cell Mol Med 2009; 13: 3720-3729.
[11] Coffelt SB, Lewis CE, Naldini L, Brown JM, Ferrara N and De Palma M. Elusive identities and overlapping phenotypes of proangiogenic myeloid cells in tumors. Am J Pathol 176: 1564-1576.
[12] Duda DG, Cohen KS, Kozin SV, Perentes JY, Fukumura D, Scadden DT and Jain RK. Evidence for incorporation of bone marrow-derived endothelial cells into perfused blood vessels in tumors. Blood 2006; 107: 2774-2776.
[13] Fukumura D, Ushiyama A, Duda DG, Xu L, Tam J, Krishna V, Chatterjee K, Garkavtsev I and Jain RK. Paracrine regulation of angiogenesis and adipocyte differentiation during in vivo adipogenesis. Circ Res 2003; 93: e88-97.
[14] Jaiswal N, Haynesworth SE, Caplan AI and Bruder SP. Osteogenic differentiation of purified, culture-expanded human mesenchymal stem cells in vitro. J Cell Biochem 1997; 64: 295-312.
[15] Duda DG, Fukumura D, Munn LL, Booth MF, Brown EB, Huang P, Seed B and Jain RK. Differential transplantability of tumor-associated stromal cells. Cancer Res 2004; 64: 5920-5924.
[16] Huang P, Duda DG, Jain RK and Fukumura D. Histopathologic findings and establishment of novel tumor lines from spontaneous tumors in FVB/N mice. Comp Med 2008; 58: 253-263.
[17] Dawson MR, Duda DG, Chae SS, Fukumura D and Jain RK. VEGFR1 activity modulates myeloid cell infiltration in growing lung metastases but is not required for spontaneous metastasis formation. PLoS One 2009; 4: e6525.
[18] Jain RK, Munn LL and Fukumura D. Dissecting tumour pathophysiology using intravital microscopy. Nat Rev Cancer 2002; 2: 266-276.
[19] Dawson MR, Duda DG, Fukumura D and Jain RK. VEGFR1-activity-independent metastasis formation. Nature 2009; 461: E4; discussion E5.
[20] Coussens LM, Tinkle CL, Hanahan D and Werb Z. MMP-9 supplied by bone marrow-derived cells contributes to skin carcinogenesis. Cell 2000; 103: 481-490.
[21] Kimura YN, Watari K, Fotovati A, Hosoi F, Yasumoto K, Izumi H, Kohno K, Umezawa K, Iguchi H, Shirouzu K, Takamori S, Kuwano M and Ono M. Inflammatory stimuli from macrophages and cancer cells synergistically promote tumor growth and angiogenesis. Cancer Sci 2007; 98: 2009-2018.
[22] Loges S, Schmidt T and Carmeliet P. "Antimyeloangiogenic" therapy for cancer by inhibiting PlGF. Clin Cancer Res 2009; 15: 3648-3653.
[23] Kim S, Takahashi H, Lin WW, Descargues P, Grivennikov S, Kim Y, Luo JL and Karin M. Carcinoma-produced factors activate myeloid cells through TLR2 to stimulate metastasis. Nature 2009; 457: 102-106.